Testing the Hill model of transpolar potential with Super Dual Auroral Radar Network observations

S. G. Shepherd,[1] J. M. Ruohoniemi,[2] and R. A. Greenwald[2]

Received 3 May 2002; revised 28 June 2002; accepted 31 July 2002; published 2 January 2003.

[1] We use a data set consisting of periods for which the transpolar ionospheric potential (Φ_{pc}) is well-determined by Super Dual Auroral Radar Network (SuperDARN) data to test the Hill model. The Hill model, as formulated by *Siscoe et al.* [2002], specifies Φ_{pc} as a function of solar wind speed and ram pressure, the interplanetary magnetic field, the reconnection electric field (E_r), and the ionospheric conductance (Σ). The periods used in our study were identified as times when the interplanetary electric field was quasi-stable for and SuperDARN coverage was sufficient to determine Φ_{pc}. SuperDARN-determined Φ_{pc} (Φ_{pc}^{SD}) is compared to Φ_{pc} determined using the Hill model (Φ_{pc}^{Hill}) for 1317 10-min periods. A minimum in the root-mean-square difference between $(\Phi_{pc}^{SD})(E_r)$ and $(\Phi_{pc}^{Hill})(E_r)$ is achieved when Σ = 23 S and a constant potential, Φ_0 = 17 kV, are used. Some aspects of the data agree very well for these values of Σ and Φ_0, including the mean value of $\Phi_{pc}(E_r)$ and that both data sets clearly indicate saturation at higher values of E_r. The ram pressure dependence of (Φ_{pc}^{Hill}), however, is inconsistent with that of (Φ_{pc}^{SD}) and suggests that Σ should be lower than 23 S. There is also significantly more variability in (Φ_{pc}^{SD}) for all values of E_r than the Hill model predicts. *INDEX TERMS:* 2463 Ionosphere: Plasma convection; 2431 Ionosphere: Ionosphere/magnetosphere interactions (2736); 2784 Magnetospheric Physics: Solar wind/magnetosphere interactions; 2437 Ionosphere: Ionospheric dynamics; 2411 Ionosphere: Electric fields (2712). **Citation:** Shepherd, S. G., J. M. Ruohoniemi, and R. A. Greenwald, Testing the Hill model of transpolar potential with Super Dual Auroral Radar Network observations, *Geophys. Res. Lett.*, *30*(1), 1002, doi:10.1029/2002GL015426, 2003.

1. Introduction

[2] The transpolar potential or cross polar cap potential (Φ_{pc}) is the total variation in the high-latitude ionospheric electric potential and is an important indicator of the amount of energy flowing into and through the magnetosphere-ionosphere (M-I) system. It is a convenient parameter often used to compare different methods of calculating electric fields in the high-latitude ionosphere.

[3] Many techniques have been developed to determine a relationship between the upstream solar wind and interplanetary magnetic field (IMF) conditions and Φ_{pc}. Some of these include spacecraft measurements of the convecting plasma [*Heppner*, 1972; *Reiff et al.*, 1981; *Doyle and Burke*, 1983; *Rich and Hairston*, 1994; *Boyle et al.*, 1997; *Weimer*, 2001], assimilation of ground and satellite measurements such as the Assimilative Mapping of Ionospheric Electrodynamics (AMIE) technique [*Richmond and Kamide*, 1988], fitting ionospheric line-of-sight (LOS) convection velocities from ground-based radars to functional forms of the electrostatic potential [*Ruohoniemi and Baker*, 1998], and global magnetospheric modeling codes [*Fedder and Lyon*, 1987; *Raeder et al.*, 2001; *Ridley*, 2001].

[4] *Siscoe et al.* [2002] have proposed a formulation of a theoretical model, the Hill model [*Hill et al.*, 1976], which takes into account M-I coupling by Region 1 currents that act to effectively reduce the strength of the magnetic field at the magnetopause merging region as the solar wind electric field (E_{sw}) increases. The resulting feedback limits the amount of reconnection at the dayside magnetopause thereby limiting the magnitude of Φ_{pc}, a behavior known as saturation [e.g., *Russell et al.*, 2001]. *Siscoe et al.* [2002] compared the Hill model with results from a global magnetospheric MHD model, the Integrated Space Weather Model (ISM), and found good agreement in terms of both Region 1 currents and Φ_{pc}. In this letter we report the first test of the transpolar potential from the Hill model (Φ_{pc}^{Hill}) against direct measurements of the potential from Super Dual Auroral Radar Network (SuperDARN) observations (Φ_{pc}^{SD}).

2. Procedure

[5] *Shepherd et al.* [2002] identified quasi-stable periods of the Kan–Lee electric field, $E_{KL} \equiv VB_T \sin^2(\theta/2)$, where V is the solar wind speed, B_T is the transverse IMF; $BT = (B_y^2 + B_z^2)^{\frac{1}{2}}$, and θ is the IMF clock angle; $\cos^{-1}(B_z/B_T)$ [*Kan and Lee*, 1979]. We break from tradition at this point and change notation from E_{KL} to E_r. The reason for our switch is that *Sonnerup* [1974] first correctly demonstrates that the upper limit of the reconnection electric field is proportional to $\sin^2(\theta/2)$ and attributed this dependence to *Petschek* [1964, 1966] and *Nishida and Maezawa* [1971]. We therefore chose to refer to the quantity $V B_T \sin^2(\theta/2)$ as the reconnection electric field, E_r.

[6] The periods identified by *Shepherd et al.* [2002] were observed by the Advanced Composition Explorer (ACE) between February 1998 and December 2000, and were required to be stable with respect to E_r to within a specified degree for $\geq$40 min. The reason for the stability criteria was to minimize the impact of the inherent uncertainties in predicting the lag time of observation of the solar wind and IMF at ACE to impact in the high-latitude ionosphere [e.g., *Ridley et al.*, 1998]. A further attempt was made to

[1]Thayer School of Engineering, Dartmouth College, Hanover, New Hampshire, USA.
[2]Johns Hopkins University, Applied Physics Laboratory, Laurel, Maryland, USA.

0094-8276/03/2002GL015426$05.00

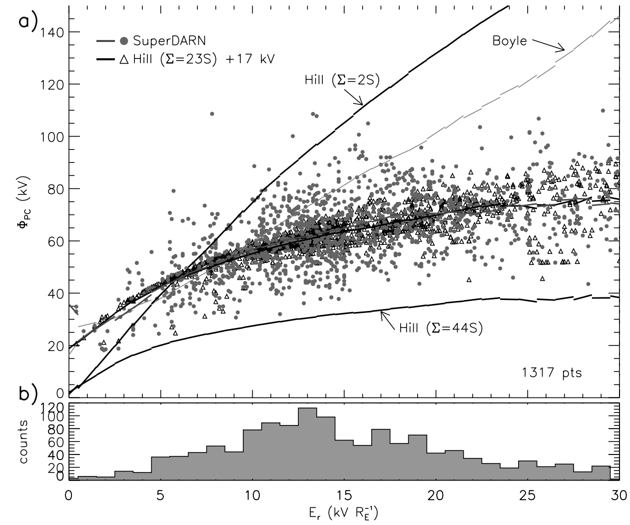

Figure 1. (a) Φ_{pc} determined using APL Fit (Φ_{pc}^{SD}) and the best-fit Hill model (Φ_{pc}^{Hill}, shown in Figure 4b) plotted against E_r. A linear fit to a 5-kV R_E^{-1} window is shown for these data and for several other comparison models: the Boyle model, $\Phi_{pc}^{Hill}(\Sigma = 2S)$, and $\Phi_{pc}^{Hill}(\Sigma = 44S)$. (b) Distribution of events in E_r.

minimize this impact by throwing out the first and last 10-min periods of each ≥40-min event.

[7] In addition to the stability requirement, these periods also satisfy the criterion that (Φ_{pc}^{SD}, determined using the Johns Hopkins University Applied Physics Laboratory Fitting technique or APL Fit [*Ruohoniemi and Baker*, 1998; *Shepherd and Ruohoniemi*, 2000], were suitably well-defined by the SuperDARN LOS Doppler velocity data. Further details of the selection criteria are provided by *Shepherd et al.* [2002].

[8] We use a subset of 1317 10-min periods from the *Shepherd et al.* [2002] data set for this study. Because the statistics are greatest in the range $E_r \leq 30$ kV R_E^{-1} (~4.7 mV m^{-1}), we use only the periods which fall in this range. Appropriately time lagged 10-min averages of the ACE/SWEPAM solar wind speed (V) and mass density (ρ), and the ACE/MAG IMF ($\vec{B}$) are used to derive (Φ_{pc}^{Hill}. Φ_{pc} is also computed for the Boyle model [*Boyle et al.*, 1997] for comparison. Φ_{pc} for these models are then directly compared to the SuperDARN-derived transpolar potential (Φ_{pc}^{SD}).

[9] The formulation of the Hill model we use in this study is given by *Siscoe et al.* [2002]

$$\Phi_{PC}^{Hill} = \frac{57.6 E_{sw} p^{\frac{1}{3}} F(\theta)}{p^{\frac{1}{2}} + 0.0125\xi\Sigma E_{sw} F(\theta)} \quad (1)$$

where $E_{sw} = VB_T$ is the solar wind electric field with V being the solar wind speed, B_T the transverse IMF, and p is the solar wind ram pressure. $F(\theta)$ is the IMF clock angle dependence of reconnection at the magnetopause, taken to be $\sin^2(\theta/2)$ following *Siscoe et al.* [2002]. A relation for ξ, a factor that depends on the geometry of the currents flowing into the ionosphere, is given as $4.45 - 1.08 \log \Sigma$ by *Siscoe et al.* [2002], where Σ is the ionospheric conductance and is assumed to be uniform. We note that the choice of $F(\theta)$ allows us to rewrite equation (1) as

$$\Phi_{PC}^{Hill}(\Sigma) = \frac{57.6 E_r p^{\frac{1}{3}}}{p^{\frac{1}{2}} + 0.0125\xi\Sigma E_r} \quad (2)$$

where $_{Er}$ is the reconnection electric field discussed earlier in section 2.

3. Data and Discussion

[10] Figure 1a shows Φ_{pc}^{SD} plotted against E_r as circles and Φ_{pc}^{Hill} (Σ = 23 S) + 17 kV as triangles (a best-fit solution to Φ_{pc}^{SD}). For each model a linear fit to Φ_{pc} in a 5-kV R_E^{-1} (~0.8 mV m^{-1}) window of E_r is shown for each unit value of E_r in kV R_E^{-1}. We also plot just the linear fits of several other models for comparison: $\Phi_{pc}^{Hill}(\Sigma = 2$ S), $\Phi_{pc}^{Hill}(\Sigma = 44$ S), and Φ_{pc} for the Boyle model. Figure 1b shows the distribution of E_r for the data set used in this study with a peak in the distribution near 13 kV R_E^{-1}(~2.0 mV m^{-1}). We show the mean and standard deviation of the windowed, linear fits to $\Phi_{pc}(E_r)$ in Figure 2a. Because there is a great deal of variability in Φ_{pc} (particularly in Φ_{pc}^{SD}) for nearly all ranges of E_r (Figure 2b).

[11] The two Hill models, $\Phi_{pc}^{Hill}(\Sigma = 2$ S) and $\Phi_{pc}^{Hill}(\Sigma = 44$ S), represent the minimum and maximum values of Σ used by *Siscoe et al.* [2002] and serve to illustrate the extremes of this model. Another Hill model, $\Phi_{pc}^{Hill}(\Sigma = 23$ S) + 17 kV, shown in Figure 2a and Figure 3 corresponds to the best-fit solution of $\Phi_{pc}^{Hill}(\Sigma) + \Phi_0$ to Φ_{pc}^{SD}. The linear fits to these data match nearly perfectly with those of over the entire range 0 $\geq E_r \geq 30$ kV R_E^{-1}.

[12] The reason for including the constant potential term Φ_0 in the best-fit solution is that one expects a non-zero minimum potential even for very low E_{sw}. Viscous magnetospheric convection, reconnection in the magnetotail, or ionospheric processes generally prevent Φ_{pc} from ever reaching zero. Because $\Phi_{pc}^{Hill} = 0$ for $E_{sw} = 0$, we add the constant Φ_0 to $\Phi_{pc}^{Hill}(\Sigma)$ when comparing to Φ_{pc}^{SD}, and attribute it to the effects of these processes.

[13] In order to determine the best-fit $\Phi_{pc}^{Hill}(\Sigma) + \Phi_0$ to Φ_{pc}^{SD}, total root-mean-square (RMS) differences between the two data sets were calculated in two ways. Figure 3a shows unit contours of the total RMS difference for the 1317

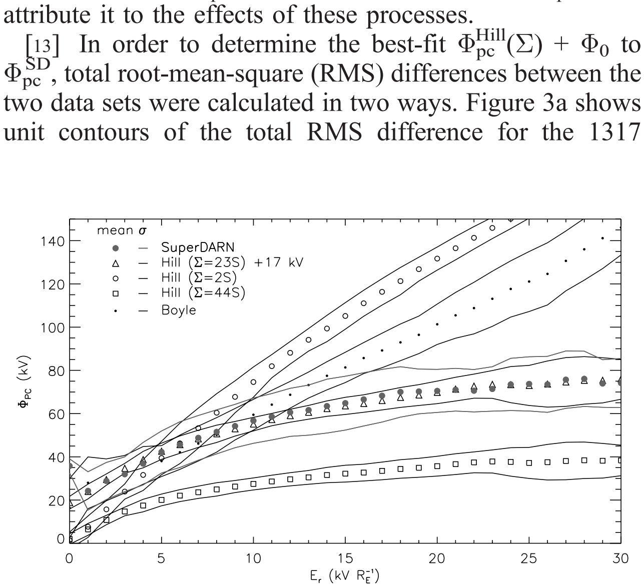

Figure 2. Φ_{pc} Mean and standard deviation of E_r-windowed, linear fits to the data shown in Figure 1a.

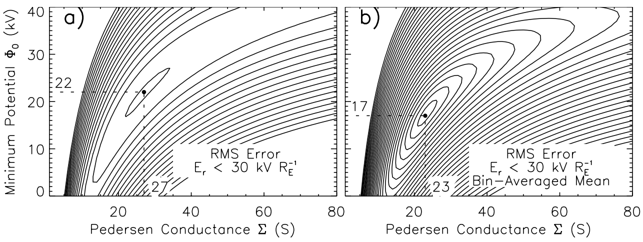

Figure 3. Unit contours of RMS differences between $\Phi_{pc}^{Hill}(E_r)$ and $\Phi_{pc}^{SD}(E_r)$, in Σ, Φ_0 space, for (a) all data points (Figures 2a and 2b) E_r-windowed, linear fits to the data (Figure 3). The minimum total RMS values are located at the intersection of the dotted lines.

periods shown in Figure 1a. This solution corresponds to a fit to all the data points. A minimum occurs when Σ = 27 S and Φ_0 = 22 kV, but it is clear that there is a family of solutions for which the RMS difference is within a few kV of this minimum. This fact is partly due to the distribution of data points shown in Figure 1b. Figure 3b shows unit contours of the total RMS difference between the E_r-windowed, linear fits shown in Figures 1a and 2a, and has a well-defined minimum. We therefore consider this, $\Phi_{pc}^{Hill}(\Sigma$ = 23 S) + 17 kV, the best-fit solution to Φ_{pc}^{SD} for these data, and note there is a possible range of solutions as shown in Figure 4a.

[14] The value of Φ_0 = 17 kV seems reasonable for the minimum transpolar potential. For this data set the lowest value of Φ_{pc} for the Boyle model is ~20 kV and the lowest value of Φ_{pc}^{SD} is ~18 kV. Some studies report Φ_0 = 22–39 kV [e.g., *Reiff et al.*, 1981] but these values were obtained by a linear fit to the data and lower values were clearly present.

[15] While Φ_0 is in good agreement with other studies, the value of ionospheric conductance, Σ = 23 S, is quite high. A typical value of uniform ionospheric conductance used in global magnetospheric MHD models is 5 S, and a few S is not unusual [e.g., *Ridley*, 2001]. Even if one considers the range of Σ for the family of solutions in Figure 4, the minimum Σ for these solutions is greater than 10 S, which is still quite high.

[16] In order to be sure that the values of Φ_{pc}^{SD} at higher values of E_r (>~15 kV R_E^{-1}) were not overly biasing the best-fit solution, RMS differences were calculated (but not shown) over the range 5 $\geq E_r \geq$ 15 kV R_E^{-1} where the statistics are greatest and values of Φ_{pc}^{SD} are most certainly well-defined [*Shepherd et al.*, 2002]. The best-fit solution for this limited range is $\Phi_{pc}^{Hill}(\Sigma$ = 20 S) + 16 kV, which is quite similar to the fit for the whole range (0 $\geq E_r \geq$ 30 kV R_E^{-1}), suggesting that Φ_{pc}^{SD} at large E_r does not bias the determination of Σ.

[17] The ram pressure dependence of Φ_{pc}^{Hill} can also be compared to that of Φ_{pc}^{SD}. Figure 4 shows $\Phi_{pc}^{SD}(p)$, the best-fit $\Phi_{pc}^{Hill}(p)$, and the two extreme-value Hill models, $\Phi_{pc}^{Hill}(\Sigma$ = 2 S) and $\Phi_{pc}^{Hill}(\Sigma$ = 44 S). The data have been binned in 5-kV R_E^{-1} intervals of E_r and plotted in Figures 4a–f along with 1-σ error bars. The horizontal dotted lines represent the average Φ_{pc}^{SD} for each range of E_r.

[18] The general trend of increasing Φ_{pc}^{SD} with increasing E_r is obvious from the panels in Figure 4. Also obvious is the lack of any Φ_{pc}^{SD} dependence on p for any range of E_r. Unlike Φ_{pc}^{SD}, Φ_{pc}^{Hill} for the best-fit solution shows a very clear p-dependence and very narrow distributions, i.e., small σs. The p-dependence becomes more pronounced at higher values of E_r. On the other hand, $\Phi_{pc}^{Hill}(\Sigma$ = 2 S) shows no p dependence and the σs are comparable to those of Φ_{pc}^{SD}, suggesting that a lower value of Σ better matches $\Phi_{pc}^{SD}(p)$. Of course, the E_r dependence of $\Phi_{pc}^{Hill}(\Sigma$ = 2 S) is inconsistent with Φ_{pc}^{SD}, i.e., the value of $\Phi_{pc}(E_r)$ is too high.

[19] One possible explanation for the relatively high value of Σ that is indicated by this comparison is that Φ_{pc}^{SD} on average is somewhat lower than inferred by some other techniques. For example, drift meter measurements from a low altitude satellite such the Dynamics Explorer-2 report that Φ_{pc} =110 kV, and possibly higher, for IMF B_z = −10 nT with solar wind speed V = 450 km s^{-1} (E_r = ~30 kV R_E^{-1}) [*Weimer*, 2001]. The mean Φ_{pc}^{SD} for this value of E_r is ~75 kV. It should be noted that Φ_{pc}^{SD} does exceed 100 kV, but there is also a great deal of variability over the entire range of E_r, perhaps causing the mean to be lower than expected.

[20] Although care was taken in selecting periods for this study, there are instances when the APL Fit technique underestimates Φ_{pc}. During extended periods of large E_r the favorable coupling between the solar wind and magnetosphere causes the lower latitude of the convection region to expand equatorward. If the convection region becomes too expanded the propagation conditions required to achieve perpendicularity and detect backscatter prevent the radars from observing the entire convection region. In this situation Φ_{pc}^{SD} underestimates the true Φ_{pc}. It is possible that some of these periods exist in our study, however, their occurrence is expected at greater frequency for larger values of E_r. Because the RMS differences over the range 5 $\leq E_r \leq$ 15 kV R_E^{-1} also suggest a higher value of Σ, it is unlikely that a systematic underestimation of Φ_{pc} due to this scenario is the sole source of the discrepancy.

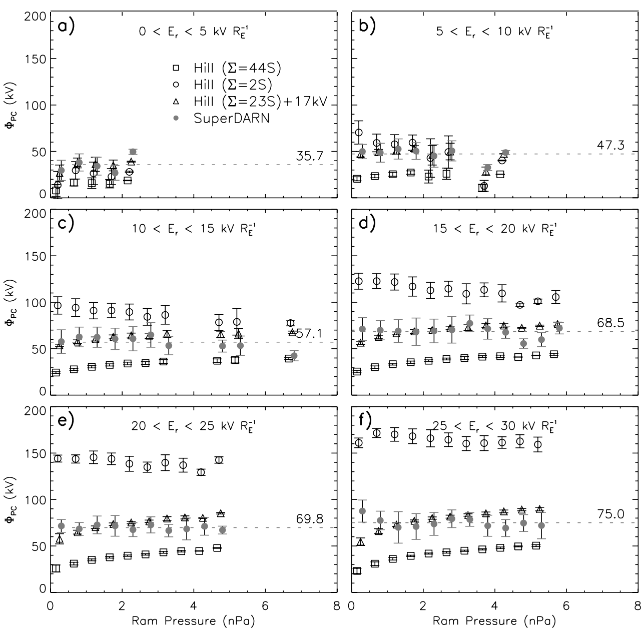

Figure 4. Ram pressure (p) dependence of Φ_{pc} for four of the models in Figure 2. The data have been binned in 5-kV R_E^{-1} intervals of E_r.

[21] Some of the variability in $\Phi_{pc}^{SD}(E_r)$ that is observed may be due to variations in the data coverage or variability in the solar wind, despite efforts to minimize uncertainties in determining Φ_{pc}^{SD} and the associated geoeffective solar wind and IMF. However, it is also possible that variability of this magnitude can only be explained by internal effects and that a model of the ionospheric potential requires detailed knowledge of the coupling between the magnetosphere and ionosphere and its time history. Another possible explanation for the relatively high value of Σ suggested by our comparison is, therefore, that the Hill model, as formulated by *Siscoe et al.* [2002], needs some modification to better match the SuperDARN results.

[22] One possibility is to adjust the parameter ξ in equation (2). *Siscoe et al.* [2002] determined the empirical expression for ξ given in section 2, from a fit to the results obtained from ISM and acknowledge that there is some flexibility in the value of this parameter. If we chose Σ =5 S and Φ_0 = 17 kV, then $\Phi_{pc}^{Hill}(\Sigma, \xi = 10) + \Phi_0$ is within 1-σ of $\Phi_{pc}^{SD}(E_r)$ for $E_r \leq 20$ kV R_E^{-1}, and within 2-σ for the entire range, $0 \leq E_r \leq 30$ kV R_E^{-1}. It is unclear whether $\xi = 10$ is a reasonable value since it is much larger than both the value of $\sim$3.7 obtained by the experimental fit and the maximum value of 4.2 used in their study. For comparison, $\Phi_{pc}^{Hill}(\Sigma = 5$ S, $\xi = 3.7) + 17$ kV is with 1-σ of $\Phi_{pc}^{SD}(E_r)$ only for $E_r \leq 4$ kV R_E^{-1}, and within 2-σ for $E_r \leq 9$ kV.

[23] It is also possible that other assumptions used to derive equation (1) are incorrect. For instance, the assumption of a uniform global conductivity may be inadequate, or the manner in which ionospheric conductivity mediates M-I coupling may need to be re-examined.

4. Conclusions

[24] We have reported on the first experimental test of the Hill model, using determinations of Φ_{pc} from SuperDARN observations. A large data set of quasi-stable IMF periods and suitable SuperDARN coverage was used to compare Φ_{pc} of the Hill model (Φ_{pc}^{Hill}) with that derived from the SuperDARN measurements (Φ_{pc}^{SD}). The Hill model incorporates feedback from the Region 1 current system and correctly predicts saturation of the transpolar potential at high values of the solar wind electric field. Comparison with Φ_{pc}^{SD}, however, reveals some discrepancies.

[25] The best-fit solution of the Hill model to $\Phi_{pc}^{SD}(E_r)$ occurs when the constant ionospheric conductance (Σ) is set to 23 S and an added minimum potential (Φ_0) is set to 17 kV. The value of Φ_0 is in reasonable agreement with the SuperDARN observations and that reported in other studies, however, the value of Σ is higher than expected. The ram pressure dependence of the Hill model also suggests that a lower value of Σ may be more appropriate. While the mean of $\Phi_{pc}^{SD}(E_r)$ is somewhat lower than reported by others, it is unlikely that a systematic underestimation of Φ_{pc} occurs over the entire range of $0 \leq E_r \leq 30$ kV R_E^{-1}, and is soley responsible for the large Σ. Most likely some of the assumptions *Siscoe et al.* [2002] used to determine equation (1) need modification.

[26] The Hill model is certainly an advance in the sophistication of representing Φ_{pc} in terms of measurable quantities. Saturation of the transpolar potential is a salient feature of this model missing in many others. Further study, however, is neccessary to determine the cause of the observed differences with the SuperDARN results.

[27] **Acknowledgments.** This work was supported by NSF grant ATM-[9812078] and NASA grant NAG5-[8361]. Operation of the Northern Hemisphere SuperDARN radars is supported by the national funding agencies of the U.S., Canada, the U.K., and France. The Hill model formulation was kindly provided by Dr. George Siscoe. We gratefully acknowledge the ACE/MAG instrument team, the ACE/SWEPAM instrument team, and the ACE Science Center for providing the ACE level 2 data.

References

Boyle, C. B., P. H. Reiff, and M. R. Hairston, Empirical polar cap potentials, *J. Geophys. Res.*, *102*, 111, 1997.

Doyle, M. A., and W. J. Burke, S3-2 measurements of the polar cap potential, *J. Geophys. Res.*, *88*, 9125, 1983.

Fedder, J. A., and J. G. Lyon, The solar wind-magnetosphere-ionosphere current-voltage relationship, *Geophys. Res. Lett.*, *14*, 880, 1987.

Heppner, J. P., Polar-cap electric field distributions related to the interplanetary magnetic field direction, *J. Geophys. Res.*, *77*, 4877, 1972.

Hill, T. W., A. J. Dessler, and R. A. Wolf, Mercury and Mars: The role of ionospheric conductivity in the acceleration of magnetospheric particles, *Geophys. Res. Lett.*, *3*, 429, 1976.

Kan, J. R., and L. C. Lee, Energy coupling function and solar wind-magnetosphere dynamo, *Geophys. Res. Lett.*, *6*, 577, 1979.

Nishida, A., and K. Maezawa, Two basic modes of interaction between the solar wind and the magnetosphere, *J. Geophys. Res.*, *76*, 2254, 1971.

Petschek, H. E., Magnetic field annihilation, The Physics of Solar Flares, *NASA Spec. Publ.*, *50*, 425, 1964.

Petschek, H. E., The mechanism for reconnection of geomagnetic and interplanetary field lines, in The Solar Wind, edited by R. J. Mackin Jr., and M. Neugebauer, pp. 257–273, Pergamon, New York, 1966.

Raeder, J., et al., Global simulations of magnetospheric space weather effects of the Bastille Day storm, *Solar Phys.*, *204*, 325, 2001.

Reiff, P. H., R. W. Spiro, and T. W. Hill, Dependence of polar cap potential drop on interplanetary parameters, *J. Geophys. Res.*, *86*, 7639, 1981.

Rich, F. J., and M. Hairston, Large-scale convection patterns observed by DMSP, *J. Geophys. Res.*, *99*, 3827, 1994.

Richmond, A. D., and Y. Kamide, Mapping electrodynamic features of the high-latitude ionosphere from localized observations: Technique, *J. Geophys. Res.*, *93*, 5741, 1988.

Ridley, A. J., Using steady state MHD results to predict the global state of the magnetosphere-ionosphere system, *J. Geophys. Res.*, *106*, 30067, 2001.

Ridley, A. J., G. Lu, C. R. Clauer, and V. O. Papitashvili, A statistical study of the ionospheric convection response to changing interplanetary magnetic field conditions using the assimilative mapping of ionospheric electrodynamics technique, *J. Geophys. Res.*, *103*, 4023, 1998.

Ruohoniemi, J. M., and K. B. Baker, Large-scale imaging of high-latitude convection with Super Dual Auroral Radar Network HF radar observations, *J. Geophys. Res., 103, 20*, 797, 1998.

Russell, C. T., J. G. Luhmann, and G. Lu, Nonlinear response of the polar ionosphere to large values of the interplanetary electric field, *J. Geophys. Res.*, *106*, 18,495, 2001.

Shepherd, S. G., and J. M. Ruohoniemi, Electrostatic potential patterns in the high latitude ionosphere constrained by SuperDARN measurements, *J. Geophys. Res.*, *105*, 23,005, 2000.

Shepherd, S. G., et al., Cross polar cap potentials measured with Super Dual Auroral Radar Network during quasi-steady interplanetary magnetic field conditions, *J. Geophys. Res.*, 107(A6), 10.1029/2001JA000152, 2002.

Siscoe, G. L., et al., Hill model of transpolar potential saturation: Comparison with MHD simulation, *J. Geophys. Res.*, 107(A6), 10.1029/2001JA000109, 2002.

Sonnerup, B. U. Ö., Magnetopause reconnection rate, *J. Geophys. Res.*, *79*, 1546, 1974.

Weimer, D. R., An improved model of ionospheric electric potentials including perturbations and application to the Geospace Environment Modeling November 24, 1996, event, *J. Geophys. Res.*, *106*, 407, 2001.

S. G. Shepherd, Thayer School of Engineering, Dartmouth College, 8000 Cummings Hall, Hanover, New Hampshire 03755-8000, USA. (simon.shepherd@dartmouth.edu)

R. A. Greenwald and J. M. Ruohoniemi, The Johns Hopkins University Applied Physics Laboratory, 11100 Johns Hopkins Road, Laurel, MD 20723. (raymond.greenwald@jhuapl.edu; mike.ruohoniemi@jhuapl.edu)